Free-Volume Distributions of Polystyrene Probed by Positron Annihilation: Comparison with Free-Volume Theories

J. Liu, Q. Deng, and Y. C. Jean*

Department of Chemistry, University of Missouri—Kansas City, Kansas City, Missouri 64110

Received June 7, 1993; Revised Manuscript Received October 8, 1993®

ABSTRACT: Positron annihilation spectroscopy has been applied to measure the free-volume hole distributions in polystyrene (T_g = 95 °C, molar weight 105 000) as a function of temperature. The hole volume distributions are determined from orthopositronium distributions. The hole volumes are distributed between 35 and 200 Å^3. The fractions of free volumes are distributed from 2.0% to 11% of total volume. The obtained free-volume distributions are compared and discussed with the experimental distributions obtained by photochromic and florescent probes and with the Turnbull–Cohen free-volume theory. The distributions of free-volume fractions fit well with the theoretical function according to the Simha–Somcynsky lattice model.

Introduction

The free-volume theory has long been proposed to explain the molecular motion and physical behavior of glassy and liquid states.[1-3] The theory has been widely adopted in the community of polymer science because it is conceptionally simple and intuitively plausible for understanding many polymer properties at a molecular level. The derived macroscopic properties from the approach of free volume at a microscopic scale are fruitful with the assistance of quantum and statistical mechanical calculations.[4] In past decades, a variety of free-volume theories[3,5-17] have been developed. In general, a simple expression of "free volume" (V_f)[4,17,18] can be written as the "total volume" (V_t) minus the "occupied volume" (V_o):

$$V_f = V_t - V_o \tag{1}$$

Different free-volume theories define V_t and V_o differently. In general, V_t has been defined more uniformly as the volume determined by the specific volume measurement. However, V_o has been defined in a variety of ways according to different theories. Cited occupied volumes include the following: (1) a calculated van der Waals excluded volume,[19] (2) the crystalline volume at 0 K,[20] and (3) the fluctuation volume swept by the center of gravity of the molecules as a result of thermal motion.[13-16] A diversity of definitions for the free volume for polymers is often seen in the literature. For example, even within a cited definition, the occupied volume has been used in various ways.[18,21] In this work, we follow the general concept of the free volume[6-11] as an open space that is freely moving in a medium. The fraction of free volume (f_v) is then defined as the ratio of the free volume to the total volume:

$$f_v = V_f/V_t \tag{2}$$

Because of the different ways of defining the free volume, f_v can vary by 1 order of magnitude among the existing theories.

One of the focused issues in polymer research is in quantifying the relationship between the molecular motion and free-volume properties. In the early stage of development, the free volume was merely thought to be a theoretical concept that could not be measured directly. It could only be deduced from other indirect measurements, such as specific volume experiments,[23] or from theoretical model calculations, such as the van der Waals dimensions for molecules.[19] This is due to the intrinsic difficulties in probing the free volume, which has a size of a few angstroms and exists in a short time period ranging from 10^{-13} s and longer. In recent years, there have been a number of attempts to measure the free volume in polymers. Small-angle X-ray and neutron diffractions have been used to determine density fluctuations and then to deduce free-volume size distributions.[24-28] For example, in polystyrene, a free volume of range 4–4000 Å^3 with a maximum of ~30 Å^3 has been reported.[27] And in poly(methyl methacrylate),[26] a mean free volume of 105 Å^3 was obtained. A photochromic labeling technique by site-specific probe has been also developed[29-35] to monitor the rate of photoisomerizations of characterized probe and to deduce the free-volume distributions. For example, in an epoxy/diamine network, an average volume of ~1000 Å^3 has been reported.[30] The technique of photoisomerization of florescent probes has been also used to observe the effect of local free-volume distribution on physical aging and molecular weight.[32-35] For different molar weights of polystyrene, the distribution of free volume ranges from 100 to 300 Å^3.[32]

Positron annihilation spectroscopy (PAS) is another microprobe that has been developed to directly determine the local free-volume hole properties in polymeric materials.[36] In this technique,[37] one employs the anti-electron, the positron, as a probe and monitors the lifetime of the positron and positronium, Ps (a bound atom which consists of an electron and the positron) in the polymeric materials under study. Because of the positive-charged nature of the positron, the positron and Ps are repelled by the core electrons of polymers and trapped in open spaces, such as holes, the free volume, and voids. The annihilation photons come mainly from these open spaces. Results of positron annihilation lifetime (PAL) measurements as a function of temperature,[38] pressure,[39] time of aging,[40] and degree of crystallinity[41] give evidence that the positron and Ps are localized in these preexisting local holes and the free volume in polymers. Because of the relatively small size of the Ps probe (1.06 Å) compared to other probes, PAS is particularly sensitive to small holes and a free volume of angstroms in size and at a time of molecular motion from 10^{-10} s and longer. In contrast to other methods, PAS is capable of determining the holes and free volume in a polymer with no significant interference

® Abstract published in *Advance ACS Abstracts*, December 1, 1993.

0024-9297/93/2226-7149$04.00/0

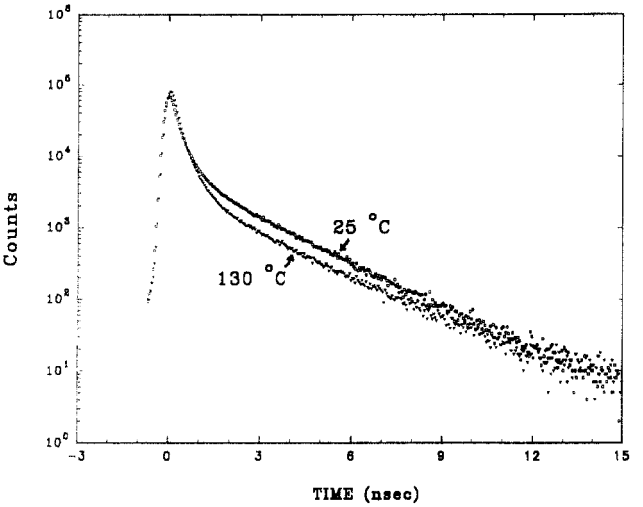

Figure 1. Temperature dependence of polystyrene PAL spectra. Raw positron lifetime spectra of polystyrene at 25 and at 130 °C. The total counts for each spectrum are 15 × 10^6.

related to the bulk. For example, in an epoxy/amine polymer, the distributions of free volume have been reported between 20 and 140 Å^3 as a function of temperature and of pressure.[42,43] The size of the free volume reported by PAS is known to be smaller than that reported by the photochromic technique.[30] The purpose of this work is to compare the distribution of free volumes obtained by PAS in polystyrene for which theoretical[11,21] and other experimental[32] distributions are available in the literature.

Experiments

1. Polystyrene Samples. The sample of polystyrene was supplied from Imperial Chemical Inc. (Wilmington, DE). The sample has an average molar weight of 105 000 and the M_W:M_N ratio is 1.1. The T_g of the sample was determined to be 95 °C from differential scanning calorimetry (DSC; Polymer Labs). The structure of polystyrene was atactic. The sample was quenched in an ice bath after it was heated at 150 °C. The size of two pieces of samples was 1 cm^2 with a thickness of 2 mm. The positron source (10 μCi of ^{22}NaCl) was directly deposited on the surface of one sample. The assembled samples and positron source were sealed in a quartz tube under vacuum. The temperature of the samples was controlled and regulated by a liquid circulator (Lauda Model SR6) within ±0.1 °C for the PAL measurements.

2. Positron Annihilation Lifetime (PAL) Spectroscopy. The positron annihilation lifetimes of polystyrene are determined by detecting the prompt γ-ray (1.28 MeV) from the nuclear decay that accompanies the emission of a positron from the ^{22}Na radioisotope and the annihilation γ-rays (0.511 MeV). A fast–fast coincidence circuit of the PAL spectrometer with a lifetime resolution of 260 ps as monitored with a ^{60}Co source was used to record all PAL spectra. Several spectra ((1–20) × 10^6 counts) were collected at each temperature for a complete data analysis of lifetime distribution. The counting rate was ~200 counts/s. Typical PAL spectra obtained in polystyrene samples above and below T_g are shown in Figure 1.

3. Principles of Determining Free-Volume Properties. In PAL spectroscopy, the observed lifetime (τ) is the reciprocal of the integral of the positron (ρ_+) and the electron (ρ_-) densities at the site where the annihilation takes place:[37]

$$\tau = \text{constant} \times \left(\int \rho_+ \rho_- \, dr\right)^{-1} \tag{3}$$

According to eq 3, a larger hole, which has a lower average electron density, is expected to have a longer Ps lifetime. For example, a correlation between the free volumes in molecular systems and the observed o-Ps lifetimes has been formulated.[44,45] This correlation is expressed in a semiempirical equation[46] between the mean o-Ps (triplet positronium) lifetime τ_3 and the mean radius of holes, R as

$$\tau_3 = 0.5\left[1 - \frac{R}{R_o} + \frac{\sin 2\pi(R/R_o)}{2\pi}\right]^{-1} \tag{4}$$

where τ_3 and R are in the units of nanoseconds and angstroms, respectively, and $R_o = R + \Delta R$. ΔR (=1.66 Å) is the best fitting parameter between the observed o-Ps lifetimes and known mean hole radii in porous materials. Although the above equation was derived from a crude approximation based on the particle in a sphere, it has been found most convenient in practical applications as long as the fitting parameter ΔR is obtained from a good fitting to the known pore sizes. From the above equation, one can determine the mean free-volume hole size in a polymeric material by measuring the o-Ps lifetime. However, the application of eq 4 is limited to a polymer which does not contain a Ps-chemical quenching (an effect that significantly shortens the Ps lifetime) functional group in its molecular structure, such as polystyrene and epoxy. The lifetime data obtained from the PAL spectroscopy contain information about the dimensions, distributions, and concentrations of holes, free volume, and voids. The current PAL results show that Ps is particularly sensitive to the free volume and holes with a size between 1 and 10 Å. A larger hole or voids (with a size of >10 Å) in polymers are not in the sensitive region of detection by current PAL technique.

4. Data Analysis. All PAL data were analyzed by two methods: (1) finite-term lifetime analysis and (2) continuous lifetime analysis. The finite-term analysis is a method for the determination of mean size and fraction, while the continuous lifetime analysis is for the determination of a distribution.

In the finite-term approach, an experimental datum $y(t)$ is expressed as a convoluted expression (by the symbol *) of the instrument resolution function $R(t)$ and of finite number (n) of negative exponentials:

$$y(t) = R(t) * \left(N_t \sum_{i=1}^{n} \alpha_i \lambda_i e^{-\lambda_i t} + B\right) \tag{5}$$

where N_t is the normalized total count, and B is the background. λ_i is the inverse of the ith lifetime component (τ_i), and $\alpha_i\lambda_i$ is its intensity. To analyze the data properly, the number of decay terms (n) for the positron annihilation needs to be assumed. The exact resolution $R(t)$ is unknown but is often approximated by a linear combination of Gaussian-type functions. The experimental data $y(t)$ are then least-squares fitted to eq 5 to obtain the fitting parameters λ_i and α_i. A computer program, PATFIT,[47] is employed for this purpose.

When three lifetimes (n = 3 in eq 5) are resolved, each lifetime corresponds to the average annihilation rate of a positron in a different state: the shortest lifetime ($\tau_1 \simeq 0.12$ ns) is due to singlet parapositronium (p-Ps), the intermediate lifetime ($\tau_2 \simeq 0.40$ ns) is due to positrons and positron–molecule species, and the longest lifetime ($\tau_3 \geq 0.5$ ns) is due to o-Ps localized in free-volume holes. In finite-term analysis, one uses a single parameter from the lifetime spectra, i.e., the longest lifetime, τ_3, to determine the mean free-volume hole size. The relative intensity corresponding to this lifetime (i.e., the o-Ps formation probability) contains information related to the number of free-volume holes. A semiempirical equation has been developed to determine the fraction of free volume (f_v) in polymers as[48]

$$f_v = AV_f I_3 \tag{6}$$

where V_f is the free volume (in Å^3) obtained from τ_3 and using eq 4 in a spherical approximation. I_3 (in %) is the o-Ps intensity, and A is a parameter which can be determined by calibrating with other physical parameters, such as with the specific volume expansion coefficients below and above T_g.[48] For example,[48] in epoxy we found that A = 0.0018 by calibrating with the volume expansion coefficients. For polystyrene, we found that A = 0.0014 by using a similar method of calibration. Equation 6 is applicable to an amorphous polymer which contains no Ps-quenching functional group in its molecular structure.[48] In common polymers, the value of A ranges from 0.001 to 0.002.

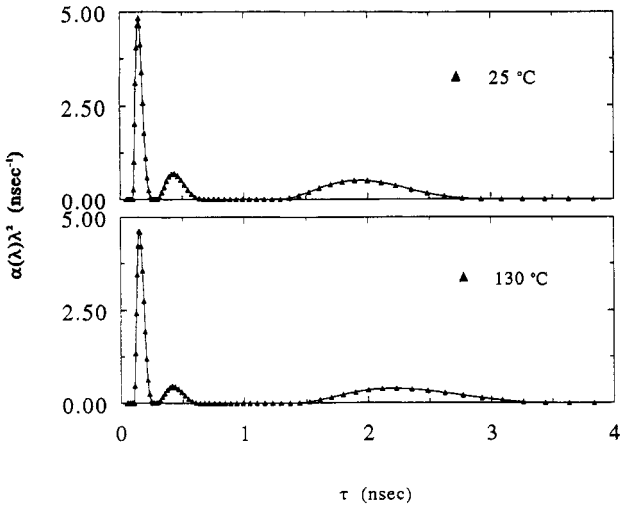

Figure 2. Lifetime distributions of polystyrene at 25 and 130 °C, respectively. The distributions were obtained by using the Laplace inversion program CONTIN.

In the continuous lifetime analysis, a PAL spectrum is expressed in a continuous decay form:[49]

$$y(t) = R(t) * (N_t \int_0^\infty \lambda\alpha(\lambda) e^{-\lambda t}\, d\lambda + B) \quad (7)$$

in which the annihilation decay integral function is simply a Laplace transformation of the decay probability density function (pdf) $\lambda\alpha(\lambda)$. The exact solution for $\alpha(\lambda)$ and λ in the above equation is a very difficult mathematical problem since the resolution function $R(t)$ is not known exactly. However, the solution can be obtained if one measures a reference spectrum from a sample with a known positron lifetime and uses it to deconvolute the unknown spectrum. For this purpose, an extra-high-purity and defect-free single crystal Cu (τ = 122 ps) was used as the reference sample. The PAL spectrum for the reference was obtained under the same experimental configurations and conditions as employed in the sample in order to preserve the same instrument resolution. The deconvolution by a Laplace inversion technique of this type was first developed by Provencher[50] into a computer code named CONTIN for the numerical solution of the integral equation. The code was later modified by Gregory and Zhu[51] for use with PAL spectra. The uniqueness in obtaining a solution by using the CONTIN program and its justification, including simulated PAL results, have been described in detail in previous papers.[51,52] For example, the Laplace inverted lifetime distributions from the PAL spectra (Figure 1) are shown in Figure 2. Three distinct peaks corresponding to p-Ps, positron, and o-Ps lifetime distributions are observed.

5. Determinations of Free-Volume Distributions. Since the o-Ps lifetime and the free-volume hole radius have a 1:1 relationship (eq 4), the continuous lifetime results contain information about the free-volume hole distributions. For clarity, we replot the o-Ps distributions (the right-hand peaks) from Figure 2 in Figure 3. An expression for the free-volume hole radius probability density function, $R\text{pdf}(R)$ has been developed as $[-\alpha(\lambda)\, d\lambda/dR]/K(R)$ to be[53]

$$R\text{pdf}(R) = -3.32\{\cos[2\pi R/(R + 1.66)] - 1\}\alpha(\lambda)/[(R + 1.66)^2 K(R)] \quad (8)$$

where $K(R)$ is the correcting factor for Ps trapping rate in different hole radii and is defined as $K(R) = 1.0 + 8.0R$. The fraction of o-Ps annihilating in the holes with radii between R and dR is $R\text{pdf}(R)\, dR$. For example, the results of $R\text{pdf}(R)$ calculated according to eq 8 and from the data in Figure 3 are shown in Figure 4. From the radius probability density function, we obtain the free-volume probability density function $V\text{pdf}(V_f)$ by assuming spherical holes as in the following equation:

$$V\text{pdf}(V_f) = R\text{pdf}(R)/4\pi R^2 \quad (9)$$

The fraction of hole volume distribution as determined by o-Ps annihilation in holes with volume between V_f and $V_f + dV_f$ is given by $V\text{pdf}(V_f)\, dV_f$. For example, the results of $V\text{pdf}(V_f)$, from the $R\text{pdf}(R)$ shown in Figure 4 and by using eq 9, are plotted in Figure 5.

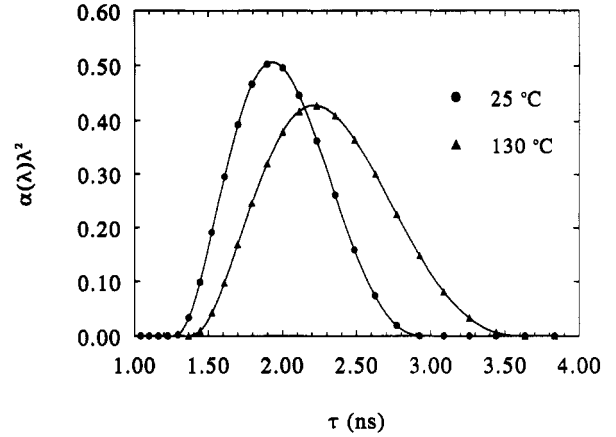

Figure 3. o-Ps lifetime distributions of polystyrene at 25 and at 130 °C. The data were taken from the right-hand peak shown in Figure 2.

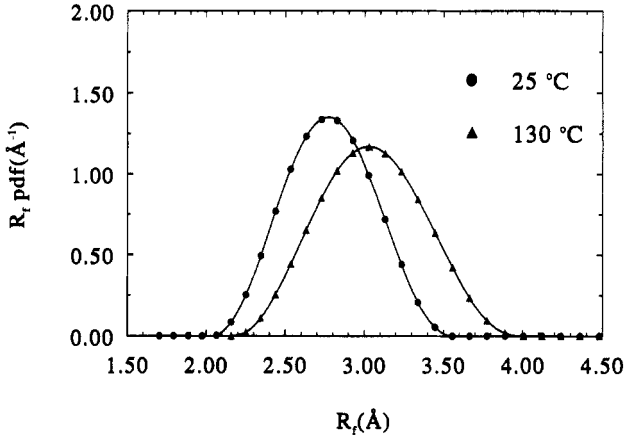

Figure 4. Free-volume hole radius distributions $R\text{pdf}(R)$ of polystyrene at 25 and at 130 °C. The distributions were calculated according to eq 8 from the data shown in Figure 3. Errors are about the size of data points. Smooth curves are drawn through data points merely for clarity.

Results and Discussion

1. Mean Free-Volume Sizes and Fractions vs Temperature. The PAL spectra in polystyrene were measured at temperatures between 25 and 130 °C at total counts between 1×10^6 and 20×10^6. The spectra were stored at an interval of every hour. The stability of the PAL spectra was carefully monitored by observing the shift of time zero (T_0) in the spectrum. Any part of the spectrum with a T_0 shift exceeding 15 ps was discarded. Only the spectra collected at a stable experimental condition are considered good data and reported here. Table I lists the results of three lifetime analyses for the spectra recorded at different temperatures. Both RESOLUTION and POSITRONFIT programs in the PATFIT package[47] were employed for data analysis.

Our PAL results listed in Table I are consistent with the existing lifetime results in polystyrene.[54-58] Particularly, the o-Ps lifetime and its intensity at ambient temperature agree very well with the results reported in a quenched sample of polystyrene with an atactic structure.[57] It is known that the o-Ps lifetime and intensity increase as the molar weight (M_W) decreases,[54] particularly at M_W below 50 000. When M_W exceeds 90 000, the o-Ps lifetime becomes constant. Our τ_3 = 2.04 ns and I_3 = 40%

Table I. Positron and Positronium Lifetime Results Obtained by Finite-Term Analysis in a Polystyrene

temp (°C)	τ_1 (ps)	τ_2 (ps)	τ_3 (ps)	T_1 (%)	I_2 (%)	I_3 (%)	$\bar{R}^b$ (Å)	f_v^c (%)
25	120 ± 0	398 ± 5	2040 ± 9	22.00 ± 0.37	37.86 ± 0.31	40.13 ± 0.24	2.88 ± 0.09	5.7 ± 0.1
50	120 ± 0	395 ± 5	2045 ± 9	18.77 ± 0.42	40.46 ± 0.35	40.78 ± 0.22	2.89 ± 0.08	5.8 ± 0.1
75	120 ± 0	388 ± 5	2053 ± 9	20.52 ± 0.43	38.85 ± 0.36	40.63 ± 0.22	2.89 ± 0.08	5.8 ± 0.1
90	120 ± 0	384 ± 4	2052 ± 8	19.48 ± 0.44	39.51 ± 0.36	41.00 ± 0.21	2.89 ± 0.08	5.8 ± 0.1
100	120 ± 0	378 ± 5	2055 ± 8	20.25 ± 0.45	38.83 ± 0.38	40.91 ± 0.21	2.90 ± 0.08	5.9 ± 0.1
110	120 ± 0	398 ± 6	2080 ± 9	24.31 ± 0.44	34.79 ± 0.36	40.90 ± 0.24	2.92 ± 0.09	6.0 ± 0.1
130	120 ± 0	396 ± 6	2106 ± 9	24.36 ± 0.43	34.94 ± 0.36	40.70 ± 0.23	2.94 ± 0.08	6.1 ± 0.1

[a] τ_1 were fixed to 120 ps, which corresponds to the p-Ps lifetime in the data analysis by using the PATFIT program. [b] $\bar{R}$ are the mean free-volume hole radii obtained by using τ_3 according to eq 4. [c] f_v are the average free-volume fractions calculated according to eq 6.

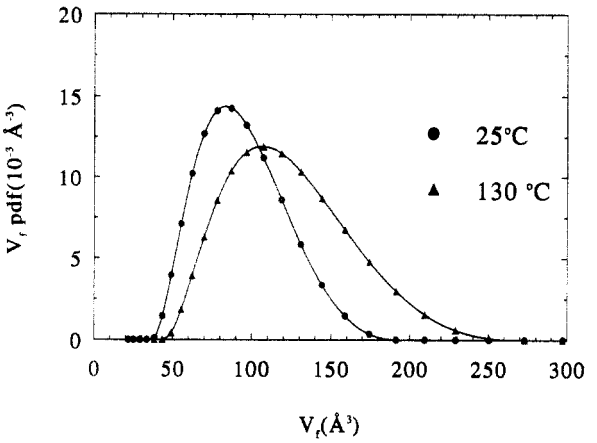

Figure 5. Free-volume distributions Vpdf(V_f) of polystyrene. Smooth curves are drawn through data points merely for clarity. The distributions were calculated according to eq 9 from the data shown in Figure 4. Errors are about the size of data points. Smooth curves are drawn through data points merely for clarity.

(M_W = 105 000) agree well with the existing values for M_W > 90 000.[54,57] The constant o-Ps lifetime implies that the size of the free volume does not increase when M_W exceeds 90 000. This result from PAL is also consistent with the constant free-volume results reported by photochromic probes in polystyrene as a function of M_W.[32]

The mean radii and fractions of free-volume holes are calculated according to eqs 4 and 6, respectively. The results are listed in Table I. Our results of mean radii (ca. 3 Å) from PAL are smaller than those reported by photochromic probe (ca. 4.2 Å).[32] On the other hand, our results of average fractions of free volume (5.7–6.1%) agree surprising well with the theoretical fractions (5.2–7.5%) calculated by Robertson[21,22] according to the Simha–Somcynsky free-volume cell model.[13]

The temperature variations of o-Ps lifetime and intensity are plotted in Figure 6. As expected, at temperatures below T_g, there is very little lifetime–temperature variation and the steepest change of τ_3 coincides with T_g (95 °C) as that found in most polymeric systems.[36] The coefficient of τ_3 with respect to temperature shown in Figure 6 is calculated to be 7×10^{-4} K^{-1}. This temperature coefficient above T_g is nearly the same as the volume expansion coefficient (6×10^{-4} K^{-1}).[23] This finding is very different from that in thermosetting polymers. For example, in epoxy systems,[38] we found that the temperature coefficient of τ_3 (6×10^{-3} K^{-1}) above T_g is 1 order of magnitude larger than the total volume expansion coefficients (5×10^{-4} K^{-1}). It appears to be a general experimental fact that the τ_3 temperature coefficient is much less in thermoplastics than in thermosetting polymers. One possible reason is that in thermoplastic materials there are additional free volumes and holes in the interfacial regions that also trap Ps. This is indicated by the fact that the observed o-Ps lifetime in thermoplastics is distributed wider and at a longer lifetime than that in thermosetting materials. More systematic

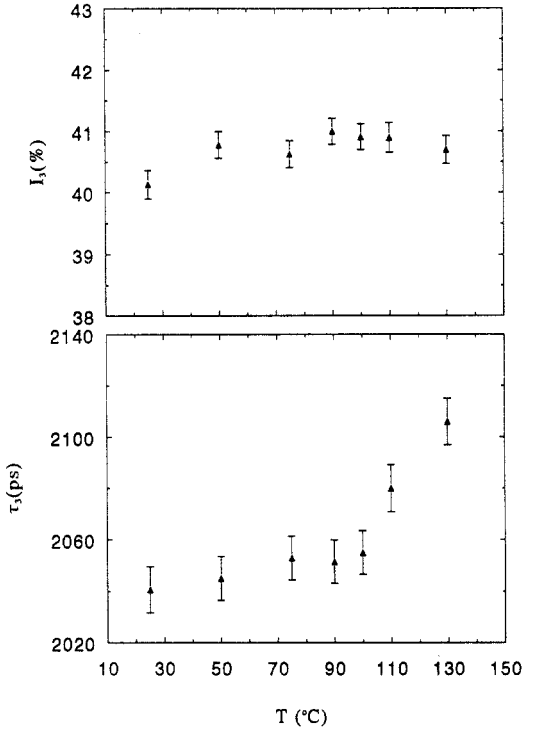

Figure 6. Mean o-Ps lifetimes and intensities as a function of temperature. These data were listed in Table I.

studies on the temperature variations of o-Ps lifetime in different types of polymeric materials are needed to understand this difference.

2. Free-Volume Distributions vs Temperature. The PAL spectra obtained at temperatures between 25 and 130 °C with higher statistics (15×10^6) were converted into continuous lifetime distributions by using the CONTIN program. The obtained o-Ps distributions are converted to radius and free-volume distributions according to eqs 8 and 9, respectively. The deconvoluted free-volume probability density distributions as a function of temperatures are shown in Figure 7.

As seen in Figure 7, the distribution of free volume shifts from a small to a larger size as the temperature increases. The distribution also becomes broader as the temperature increases above T_g. There exists a critical volume V_c. Below V_c there is no detectable free volume by current PAL technique. For examples, V_c = 35 Å^3 and V_c = 43 Å^3 are found at 25 and 130 °C, respectively. The mean free volumes, by integrating the distributions from data in Figure 7, are found to be 90 and 115 Å^3 25 and 130 °C, respectively. These free volumes are consistent with the results obtained by the finite-term analysis as listed in Table I. Detailed comparisons in the mean lifetime results obtained by using the finite-term and the continuous analysis methods for PAL spectra have been carefully examined in our previous papers.[42,43] New information from the continuous lifetime analysis is the distribution of free-volume holes. Comparing the free-volume distri-

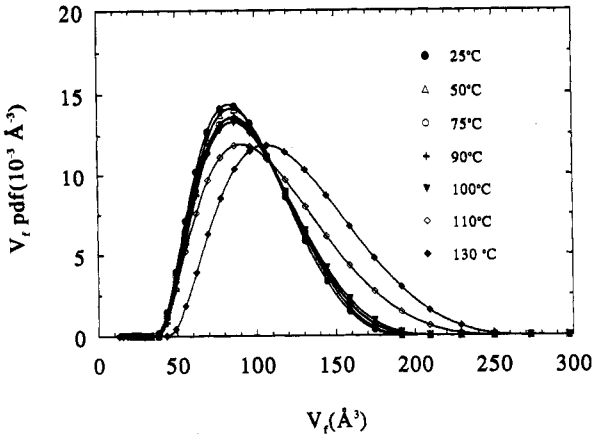

Figure 7. Free-volume distributions $V\text{pdf}(V_f)$ of polystyrene (T_g = 95 °C) at different temperatures. Errors are about the size of data points shown. Smooth lines are drawn through data points for clarity.

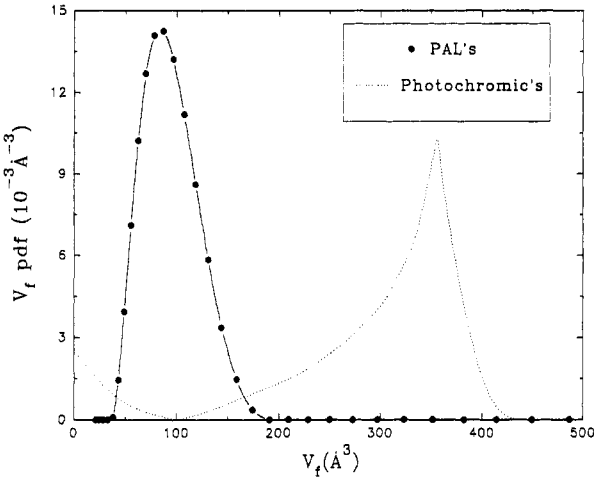

Figure 8. Comparisons of free-volume distributions obtained by PAL and from photochromic probes. PAL results are from the current work and the photochromic results were taken from ref 32. Errors for PAL results are about the size of data points.

butions of polystyrene with those in epoxy,[41] we found the distributions in polystyrene are wider. This wider distribution in polystyrene may be due to additional distribution of free volume in between the interfacial regions in thermoplastic materials.

3. Comparisons with Photochromic Experiments and with the Turnbull–Cohen Theory. The size distribution of local free volume in polystyrene has been reported by using photochromic and florescent probe studies.[31,32] In Figure 8, we compare the distributions of free volume in polystyrene obtained by PAL and by photochromic probes. The distribution from the photochromic probe below 100 Å^3 shown in Figure 8 is probably not real because it was extrapolated from data above 120 Å^3.[32] Neglecting this part of the distribution and comparing it with the current PAL results, we have the following observations: (1) The distribution from PAL is at a smaller volume than that from photochromic probes. (2) The distribution is narrower from PAL than from photochromic probes, particularly at the smaller volume. (3) The shapes of distribution at the larger volume between PAL and photochromic probes are similar.

From these observations, we found that the sensitive regions of detecting volume distributions between PAL and photochromic probes are different. PAL appears to be more sensitive to a smaller volume while the photochromic probes are more sensitive to a larger free volume.

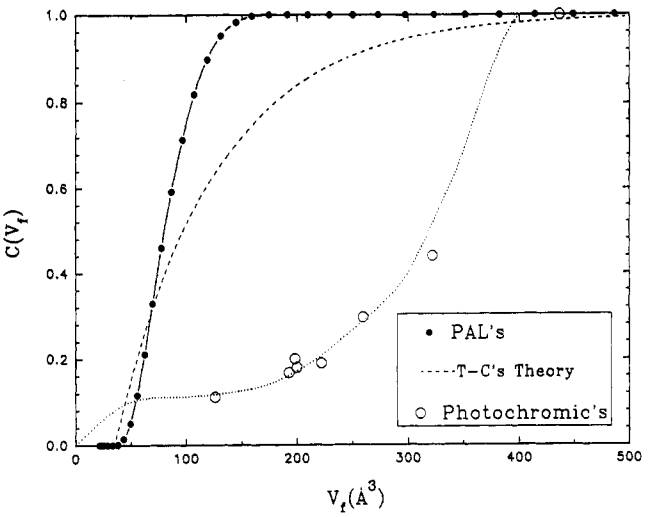

Figure 9. Comparisons of the cumulative distributions of free volume in polystyrene. The PAL results are from the current work, the photochromic results are taken from ref 32, and the theoretical distribution is according to the Turnbull–Cohen theory.[6-11] Errors are about the sizes of data points.

Ps in PAL has a size of 1.06 Å, which is much smaller than those characterizing molecules (with a size ca. 3–10 Å) used in the photochromic method. On the other hand, as shown in Figure 8, it is surprising that almost no distribution of free volume between 200 and 400 Å^3 is detected by the current PAL. In principle, these volumes are still in the highly sensitive detecting regions in PAL technique. Two possible explanations to this discrepancy regarding the distributions of free volume in polystyrene by two methods are as follows: (1) The actual distribution obtained by photochromic probes is shifted ~200 Å^3, or (2) the actual distribution of free volume is a combination of PAL and photochromic probes. More results from the same systems with these two probes are certainly needed to understand this discrepancy.

Next, we compare the cumulative distribution of free volume between these two probes with the theoretical distribution according to the Turnbull–Cohen theory.[6-8] We calculate the cumulative distribution $C(V_f)$ according to the equation

$$C(V_f) = \int_0^{V_f} V\text{pdf}(V_f)\, dV_f \qquad (10)$$

where $V\text{pdf}(V_f)$ is the free-volume distribution function obtained from PAL experiments. The results of $C(V_f)$ from the PAL data are plotted in Figure 9. The experimental data from photochromic probes[32] are also plotted in Figure 9. Comparing these experimental cumulative distributions, we found a similar discrepancy exists between them as those observed in the distributions (Figure 8). According to the Turnbull–Cohen free-volume theory, Crest and Cohen[9-11] associated the free volume with each flexible segment of a polymer molecule in a liquid-like cell model and derived the distribution probability of the local free volume to be an exponential function. The derived cumulative distribution for the free volume larger than V_f according to this theory is expressed as[10,11]

$$C(V_f) = 1 - \exp[-(V_f - V_c)/V_m] \qquad (11)$$

where V_c is the critical volume for a glass occurring in a liquid-like motion and V_m is the mean free volume. To compare the cumulative distributions with the PAL results, we take V_c and V_m from the experimental results of V_f distributions as the minimal and average V_f, respectively.

From the PAL data shown in Figure 7, V_c = 35 Å^3 and V_m = 90 Å^3 at 25 °C. The theoretical distribution of eq 11 is then plotted in Figure 9 to compare with the experimental cumulative distributions. As shown in Figure 9, in the small volume, experimental $C(V_f)$ follows the exponential distribution derived by the theory. But it deviates from the theoretical curve when the volume is large, particularly when the volume exceeds 100 Å^3. This is another indication that the free-volume results from PAL are more accurate for the small volumes where molecular relaxation takes a longer time. The discrepancy at the larger volumes between the Turnbull–Cohen theory and PAL experiments can be partly due to the limit of detecting any volume formed at a time shorter than the annihilation lifetime of the positron in polymers (i.e., 10^{-10} s). On the other hand, as seen in Figure 9, the results of $C(V_f)$ from photochromic probes have deviated far from the function according to the Turnbull–Cohen theory. This is indicates that the actual free volumes determined by photochromic probes would have shifted too large by ~200 Å^3 in polystyrene.

4. Comparison with the Simha–Somcynsky Theory. The free volume for the equilibrium state theory derived by Simha and Somcynsky[13] has been developed very successfully in recent years for describing the pressure–temperature–volume relationships of polymers.[14-16,21-22,25] This theory is based on a cell (lattice) model. The free volume is set equal to the fraction of unoccupied cells obtained by minimizing the Helmholtz free energy. The fraction of free volume and its distribution can be calculated according to a stochastic model by assuming that the free volume is distributed with some parameters related to the equation of state.[15,16,21,22] An expression of the distribution of fractional free volume with two parameters of the mean and mean-square fluctuations is given according to a Γ-distribution function:[21,22]

$$f_v\text{pdf} = \chi(\chi f_v)^{\beta-1} \exp^{-\chi f_v}/\Gamma(\beta) \qquad (12)$$

where $\Gamma(\beta)$ is the gamma function and β and χ are parameters whose values are determined by the following equations for the mean and mean-square fluctuations in free volume:[21]

$$\beta/\chi = f_m; \quad \beta/\chi^2 = \langle \Delta f_v^2 \rangle_m \qquad (13)$$

The normalized distributions of fractional free volume $f_v$pdf for a given polymer can be computed by assuming some kinetic parameters of the system. For example, in polystyrene, critical parameters of pressure (p^* = 7453 bar), temperature (T^* = 12 680 K), and volume (V^* = 0.9598 cm^3/g) have been obtained by fitting the volume recovery data.[21,22] To compute $f_v$pdf for polystyrene, three computer programs from ref 21 are used. For the current system, we have used T_g = 95 °C, and the number of segments in forming a free-volume hole, N_s = 40. The computed $f_v$pdf according to eqs 12 and 13 in polystyrene at 25 and 130 °C are plotted in Figure 10. The values computed are f_m = 0.0524 and 0.0753 and $\langle \Delta f_v^2 \rangle_m$ = 2.38 × 10^{-4} and 3.31 × 10^{-4} for the temperatures at 25 and 130 °C, respectively.

In order to compare the PAL free-volume distributions with the theoretical fractional distributions, we convert the V_f and $V_f$pdf to f_v and $f_v$pdf by using eq 6 and the following equation:

$$f_v\text{pdf} = V_f\text{pdf}V_{norm} \qquad (14)$$

where V_{norm} is the normalized factor between the integral of total free volume and the fraction of free volume from PAL experiments. V_{norm} are found to be 1840 and 1875 Å^3 at 25 and 130 °C, respectively. The obtained results of $f_v$pdf vs f_v from PAL experiments are plotted in Figure 11.

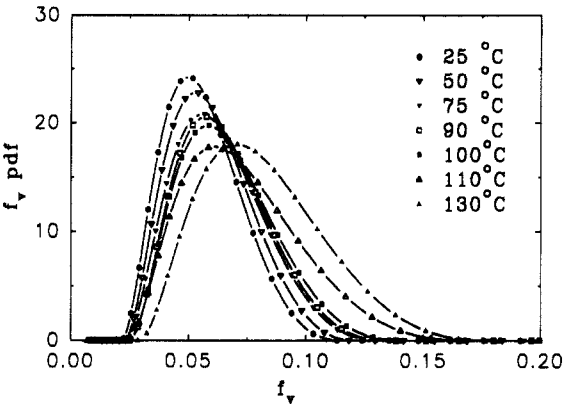

Figure 10. Distributions of free-volume fractions $f$pdf in polystyrene (T_g = 95 °C) at different temperatures. Errors are about the sizes of data points shown. Smooth lines are drawn through data points for clarity.

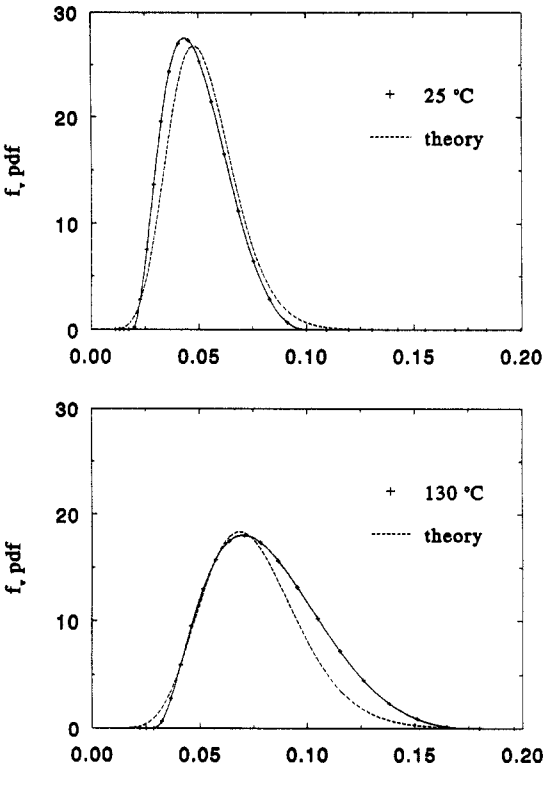

Figure 11. Comparisons of the distributions of free-volume fractions $f$pdf(f) in polystyrene between theory and experiment. Solid lines are drawn through the experimental data from the current PAL studies and dashed lines are the theoretical distributions according to the Simha–Somcynsky cell model.[13-16,21-22]

Comparing the experimental and theoretical distributions, we found the agreements are amazing good in spite of various approximations embedded in both theory and the experimental methods. The Γ-distribution function appears to be a better function than the exponential function for the fractional free-volume distribution. Since the Simha–Somcynsky theory was derived from the liquid state, as shown in Figure 11, the experiments agree with the theory even better for the liquid state than the glassy state, particularly at a small fraction of free volume. There exists a larger deviation for the larger fraction in the liquid

state but less in the glassy state. For the larger fraction, the time of molecular motion could be very short because the creation of a hole involves a smaller number of segments in a polymer. Although the deviation between theory and experiments is small, the relatively larger deviation between them is seen in Figure 11 for the larger fractions. We have further tested the theory by varying the number of monomers involved in forming a free-volume hole (N_S) from 20 to 50. The results show very small difference in the distributions as N_S varies in these numbers. Therefore, in the Simha–Somcynsky free-volume theory, $N_S > 20$ appears to be adequate to describe the free-volume distribution in polystyrene. This result is consistent with other results based on computer-simulated PAL spectra in the polycarbonate system.[59,60]

Conclusion

We have reported the distributions of free volume and fractions in a polystyrene polymer as a function of temperature by using the PAL technique. Quantitative comparisons on the distributions of free volume have been made for the first time on the results obtained by the PAL and photochromic methods. The free-volume results from PAL experiments are found to be consistently smaller than that from the photochromic and florescent probes. The obtained free-volume distributions at the small volumes are found to be describable by the exponential function according to the Turnbull–Cohen theory but to deviate significantly at the larger volumes. The fractional distributions of free volume are found to follow the Γ-distribution function and fit well with the Simha–Somcynsky cell model in both glass and liquid states.

Acknowledgment. This work has been supported by a grant from the National Science Foundation (DMR-9004083). Fruitful discussions with Profs. Simha, Robertson, and Torkelson and Dr. H. Yang are acknowledged.

References and Notes

(1) Fox, T. G.; Flory, P. J. *J. Phys. Chem.* **1951**, *55*, 211.
(2) Fox, T. G.; Flory, P. J. *J. Appl. Phys.* **1951**, *21*, 581.
(3) Doolittle, A. K. *J. Appl. Phys.* **1951**, *22*, 1471.
(4) For example, see: Ferry, J. D. *Viscoelastic Properties of Polymers*, 3rd ed.; John Wiley & Son: New York, 1980.
(5) Williams, M. L.; Landel, R. F.; Ferry, J. D. *J. Am. Chem. Soc.* **1955**, *77*, 3701.
(6) Cohen, M. H.; Turnbull, D. *J. Chem. Phys.* **1959**, *31*, 1164.
(7) Turnbull, D.; Cohen, M. H. *J. Chem. Phys.* **1961**, *34*, 120.
(8) Turnbull, D.; Cohen, M. H. *J. Chem. Phys.* **1970**, *52*, 3038.
(9) Cohen, M. H.; Grest, G. S. *Phys. Rev. B* **1979**, *20*, 1077.
(10) Cohen, M. H.; Grest, G. S. *N.Y. Acad. Sci.* **1981**, *77*, 199.
(11) Grest, G. S.; Cohen, M. H. *Adv. Chem. Phys.* **1981**, *48*, 455.
(12) Raudell, R. W.; Ngai, K. L.; Fong, G. R.; Aklonis, J. J. *Macromolecules* **1987**, *20*, 1060.
(13) Simha, R.; Somcynsky, T. *Macromolecules* **1969**, *2*, 342.
(14) Simha, R. *Macromolecules* **1977**, *10*, 1025.
(15) Robertson, R. E.; Simha, R.; Curro, J. G. *Macromolecules* **1985**, *18*, 2239.
(16) Robertson, R. E.; Simha, R.; Curro, J. G. *Macromolecules* **1988**, *21*, 3216.
(17) Kumins, C. A.; Kwei, T. K. In *Diffusion in Polymers*; Crank, J., Park, G. S., Eds.; Academic Press: New York, 1968; p 107.
(18) Haward, R. N. *J. Macromol. Sci., Rev. Macromol. Chem.* **1970**, *C4*, 191.
(19) Bondi, A. A. *Physical Properties of Molecular Crystals, Liquids, and Crystals*; Wiley & Sons: New York, 1960.
(20) Lee, W. M. *Polym. Eng. Sci.* **1980**, *20*, 65.
(21) Robertson, R. E. In *Computational Modeling of Polymers*; Bicerano, J., Ed.; Marcel Dekker: Midland, MI, 1992; p 297.
(22) Robertson, R. E. *J. Polym. Sci. Polym. Symp.* **1978**, *63*, 173.
(23) Plazek, D. J. *J. Chem. Phys.* **1965**, *69*, 3480.
(24) Roe, R. J.; Curro, J. G. *Macromolecules* **1983**, *16*, 428.
(25) Curro, J. G.; Roe, R. J. *Polymers* **1984**, *25*, 1424.
(26) Roe, R. J.; Song, H. H. *Macromolecules* **1985**, *18*, 1603.
(27) Song, H. H.; Roe, R. J. *Macromolecules* **1987**, *20*, 2723.
(28) Nojima, S.; Roe, R. J.; Rigby, D.; Han, C. C. *Macromolecules* **1990**, *23*, 4305.
(29) Yu, W.-C.; Sung, C. S. P.; Robertson, R. E. *Macromolecules* **1988**, *21*, 355.
(30) Yu, W.-C.; Sung, C. S. P. *Macromolecules* **1988**, *21*, 365.
(31) Victor, J. G.; Torkelson, J. M. *Macromolecules* **1987**, *20*, 2241.
(32) Victor, J. G.; Torkelson, J. M. *Macromolecules* **1988**, *21*, 3490.
(33) Royal, J. S.; Victor, J. G.; Torkelson, J. M. *Macromolecules* **1992**, *25*, 729.
(34) Royal, J. S.; Victor, J. G.; Torkelson, J. M. *Macromolecules* **1992**, *25*, 4792.
(35) Meyer, E. F.; Jamieson, A. M.; Simha, R.; Palmen, J. H. M.; Booij, H. C.; Maurer, F. H. J. *Polymers* **1990**, *31*, 243.
(36) For examples, see: Jean, Y. C. *Microchem. J.* **1990**, *42*, 72. Stevens, J. R. In Probe and Label Techniques. Methods of Experimental Physics; Fava, R. A., Ed.; Academic: London, 1980; p 371.
(37) For examples, see: *Positron and Positronium Chemistry*; Schrader, D. M., Jean, Y. C., Eds.; Elsevier: Amsterdam 1988. *Positron Solid-State Physics*; Brandt, W., Dupasquier, A., Eds.; North Holland: Amsterdam, 1984.
(38) Jean, Y. C.; Sandreczki, T. C.; Ames, D. P. *J. Polym. Sci. B* **1986**, *24*, 1247.
(39) Deng, Q.; Sundar, C. S.; Jean, Y. C. *J. Phys. Chem.* **1992**, *96*, 492.
(40) Kobayashi, Y.; Zheng, W.; Meyer, E. F.; McGervey, J. D.; Jamieson, A. M.; Simha, R. *Macromolecules* **1989**, *22*, 2303.
(41) Nakanishi, H.; Jean, Y. C.; Smith, E. G.; Sandreczki, T. C. *J. Poly. Sci. B* **1989**, *27*, 1419.
(42) Deng, Q.; Zandiehnadem, F.; Jean, Y. C. *Macromolecules* **1992**, *25*, 1090.
(43) Deng, Q.; Jean, Y. C. *Macromolecules* **1993**, *26*, 30.
(44) Tao, S. J. *J. Chem. Phys.* **1972**, *56*, 5499.
(45) Eldrup, M.; Lightbody, D.; Sherwood, J. N. *Chem. Phys.* **1981**, *63*, 51.
(46) Nakanishi, H.; Wang, S. J.; Jean, Y. C. In *Positron Annihilation Studies of Fluids*; Sharma, S. C., Ed.; World Science: Singapore, 1988; p 292.
(47) PATFIT package (1989). Purchased from Risø National Laboratory, Roskilde, Denmark.
(48) Wang, Y. Y.; Nakanishi, H.; Jean, Y. C.; Sandreczki, T. C. *J. Polym. Sci. B* **1990**, *28*, 1431.
(49) Schrader, D. M. In *Positron Annihilation*; Coleman, P. G., Sharma, S. C., Diana, L. M., Eds.; North-Holland: Amsterdam, 1982; p 912.
(50) Provencher, S. W. CONTIN program, EMBL Technical Report DA05, European Molecular Biology Laboratory, Germany 1982; *Comput. Phys. Commun.* **1982**, *27*, 229.
(51) Gregory, R. B.; Zhu, Y. *Nucl. Instrum. Methods Phys. Res., Sect. A* **1990**, *A290*, 172.
(52) Jean, Y. C.; Dai, G. H. *Nucl. Instrum. Methods Phys. Sect. B* **1993**, *B79*, 356.
(53) Jean, Y. C.; Deng, Q. J. *Polym. Sci. B* **1992**, *30*, 1359.
(54) West, D. H. D.; Mcbrierty, V. J.; Delaney, F. G. *Appl. Phys.* **1975**, *7*, 171.
(55) Jain, P. C.; Bhatnager, S.; Gupta, A. *J. Phys. C, Solid State Phys.* **1972**, *5*, 2156.
(56) Bertolaccini, M.; Bisi, A.; Gambarini, G.; Zappa, L. *J. Phys. C, Solid State Phys.* **1974**, *7*, 3827.
(57) McGervey, J.; Panigraphi, N.; Simha, R.; Jamieson, A. M. In *Positron Annihilation*; Jain, P. C., Singru, R. M., Gopinathan, K. P., Eds.; World Science: Singapore, 1985; p 690.
(58) Ariov, P. U.; Vasserman, S. N.; Dontsov, A. A.; Tishin, S. A. *Dokl. Phys. Chem.* **1984**, *8*, 661.
(59) Vleeshouwers, S.; Kluin, J.-E.; McGervey, J. D.; Jamieson, A. M.; Simha, R. *J. Polym. Sci. B* **1992**, *30*, 1492.
(60) Kluin, J.-E.; Yu, Z.; Vleeshouwers, S.; McGervey, J. D.; Jamieson, A. M.; Simha, R.; Sommer, K. *Macromolecules* **1993**, *26*, 1853.